Non-linear wave packet dynamics of coherent states

J BANERJI

Physical Research Laboratory, Navrangpura, Ahmedabad 380 009, India

Abstract. We have compared the non-linear wave packet dynamics of coherent states of various symmetry groups and found that certain generic features of non-linear evolution are present in each case. Thus the initial coherent structures are quickly destroyed but are followed by Schrödinger cat formation and revival. We also report important differences in their evolution.

1. Introduction

Coherent states were first introduced by Schrödinger to describe non-spreading wave packets for harmonic oscillators. They have many interesting properties, chief among which is that these are minimum uncertainty states and, therefore, are most classical within the framework of quantum theory. In recent years, the non-linear quantum dynamics of these states have revealed some striking features. It was found that under the action of a Hamiltonian which is a *non-linear* function of the photon operator(s) *only*, an initial coherent state loses its coherent structure quickly due to quantum dephasing induced by the non-linearity of the Hamiltonian; then regains it (revival) after an interval. At fractions of this time interval, the initial coherent state breaks up into a superposition of two or more coherent states which also can have a coherent structure. This is an example of the quantum phenomenon of fractional revival [1–6], or, the formation of Schrödinger cat and cat-like states [7] which, unlike a coherent state, have many non-classical properties.

We should stress that these features are not unique to coherent states of light. In fact, they arise in the evolution of a wide variety of systems (where the initial state can be a light field, a material particle or a light-matter combination) such as light propagation in Kerr media [7], optical parametric oscillators [3], Rydberg atoms [2], particle in potential wells [8], molecular vibrational states [9] and the Jaynes–Cummings model [4].

From a group theoretic point of view, the harmonic oscillator (HO) coherent states arise in systems whose dynamical symmetry group is the Heisenberg–Weyl group. Coherent states of other symmetry groups also exist. Thus, for example, the much studied pair [10] and Perelomov [11] coherent states belong to the SU(1,1) group and are special cases of what may be called generalized SU(1,1) coherent states [12,13]. Coherent states of the SU(2) group have also been constructed [14].

Our objective is to present a comparative study of how coherent states of various symmetry groups evolve under the action of the *same* two-mode generic Hamiltonian. Through a series of pictures, we show how the initial coherent structure is lost due to quantum dephasing and then regained later on to form spectacular and varied quasi-coherent structures leading up to the formation of Schrödinger cats in some cases and to full revival in all cases.

The plan of the paper is as follows. In §2, we explain the basic concepts of revival and cat formation, introduce the HO coherent state and give an example of cat formation for a single mode case. In §3, we generalise our formalism to include two-mode cases and also coherent states of other groups. The paper ends with concluding remarks in §4.

2. Basic concepts

We start with the *number* or *Fock* states $|n\rangle$. These are eigenstates of the number operator:

$$a^\dagger a |n\rangle = n|n\rangle \quad \text{for which} \quad \langle x \rangle = \langle p \rangle = 0. \tag{1}$$

The state $|n\rangle$ contains precisely n photons.

Coherent states $|\alpha\rangle$ are a particular superposition of number states:

$$|\alpha\rangle = \exp(-|\alpha|^2/2) \sum_n \frac{\alpha^n}{\sqrt{n!}} |n\rangle, \tag{2}$$

where α can be complex. Note that $|\langle n|\alpha\rangle|^2 = \exp(-|\alpha|^2)|\alpha|^{2n}/n!$ is a Poisson distribution peaked at $n = |\alpha|^2$.

HO coherent states can be defined in three equivalent ways:

1. These are displaced vacuum states: $|\alpha\rangle = \underbrace{e^{-|\alpha|^2/2}e^{\alpha a^\dagger}e^{-\alpha^* a}}_{\text{Displacement Operator}} \underbrace{|0\rangle}_{\text{vacuum}}$.

2. These are eigenstates of the annihilation operator: $a|\alpha\rangle = \alpha|\alpha\rangle$. Since light is, in general, detected by absorption, coherent states have the nice property that they remain coherent even after detection.

3. HO coherent states are states of minimum uncertainty: $\Delta p \Delta x = \hbar/2$, and thus are most classical within the quantum framework.

Output from a well stabilised laser is a coherent state.

A *cat-like* state $|\Psi\rangle$ can be considered as a superposition of two or more coherent states and is formed when an initial coherent state $|\alpha\rangle$ is rotated in phase space by a set of angles θ_p:

$$|\alpha\rangle \longrightarrow \sum_p c_p |\alpha e^{i\theta_p}\rangle. \tag{3}$$

Since rotations in phase space conserve photon numbers, the underlying Hamiltonian for the formation of cat states should be a function of the number operator only. Cat states have highly non-classical features, such as sub-Poissonian statistics and squeezing. It is interesting to note that a superposition of quantum states $|n\rangle$ produces a coherent state $|\alpha\rangle$

which has many classical features, and a superposition of these classical-like states, in turn, produces the non-classical cat states. What makes all this happen is, of course, quantum interference.

How do we form a cat state of coherent states? Let us first consider linear evolution. If $U_L(t)$ is the evolution operator corresponding to a Hamiltonian which is linear in $a^\dagger a$: $U_L(t) = \exp(-i\omega t a^\dagger a)$, then $U_L(t)|\alpha\rangle = |\alpha \exp(-i\omega t)\rangle$. Thus the linear evolution of $|\alpha\rangle$ is a rotation in phase space. The initial state will be revived at $\omega t = 2\pi, 4\pi$ as expected, but we need a Hamiltonian *nonlinear* in $a^\dagger a$ for the formation of cat states. Let us provide an example.

2.1 *Propagation of a single mode field in a Kerr medium*

A Kerr medium is nonlinear in the sense that its refractive index n has a component which varies with the intensity of the propagating field $\vec{\epsilon}$, that is, $n = n_0 + n_2|\vec{\epsilon}|^2$, where n_0 and n_2 are constants. Silica fibres are good examples of Kerr media. For a single mode field (described by the creation and annihilation operators a, $a^\dagger$) propagating through a low-loss Kerr media, the interaction Hamiltonian can be written as

$$H = \chi a^{\dagger 2} a^2 = \chi(a^\dagger a)(a^\dagger a - 1), \tag{4}$$

where χ is the third-order nonlinear susceptibility of the medium. The number state $|n\rangle$ is an eigenstate of this Hamiltonian so that if the initial state is a coherent state

$$|\alpha\rangle = \sum_n c_n|n\rangle \quad c_n = \exp(-|\alpha|^2/2)\frac{\alpha^n}{\sqrt{n!}}, \tag{5}$$

then the state at time t will have the form

$$|\alpha(t)\rangle = \sum_n c_n e^{-i\chi t(n^2-n)}|n\rangle. \tag{6}$$

Since $n^2 - n$ is always an even number, the system will revive whenever χt is a multiple of π.

In between revivals, let $\chi t = \pi r/s$ where r, s are mutually prime with $r < s$. Then we can write the quadratic (in n) phase in terms of linear phases using *discrete Fourier transform*:

$$\exp(-i\pi r n^2/s) = \sum_{p=0}^{l-1} a_p^{(r,s)} \exp(-2\pi i p n/l), \tag{7}$$

where

$$l = \begin{cases} s, & \text{if } r \text{ is odd}, s \text{ is even or vice-versa}, \\ 2s, & \text{if both } r \text{ and } s \text{ are odd}; \end{cases} \tag{8}$$

and

$$a_p^{(r,s)} = \frac{1}{l} \sum_{k=0}^{l-1} \exp(-i\pi rk^2/s + 2\pi ipk/l). \tag{9}$$

The coefficients $a_p^{(r,s)}$ have closed-form analytic expressions [15]. Substituting in (6), we get

$$|\alpha(t)\rangle = \sum_{p=0}^{l-1} a_p^{(r,s)} |\alpha \exp\left[i\pi\left(r/s - 2p/l\right)\right]\rangle \tag{10}$$

which is a cat-like state. To visualise this, we will study the evolution of its Q function.

2.2 *The Q function and its evolution*

Coherent states satisfy the completeness relation

$$\int \frac{\mathrm{d}^2\beta}{\pi} |\beta\rangle\langle\beta| = 1 \tag{11}$$
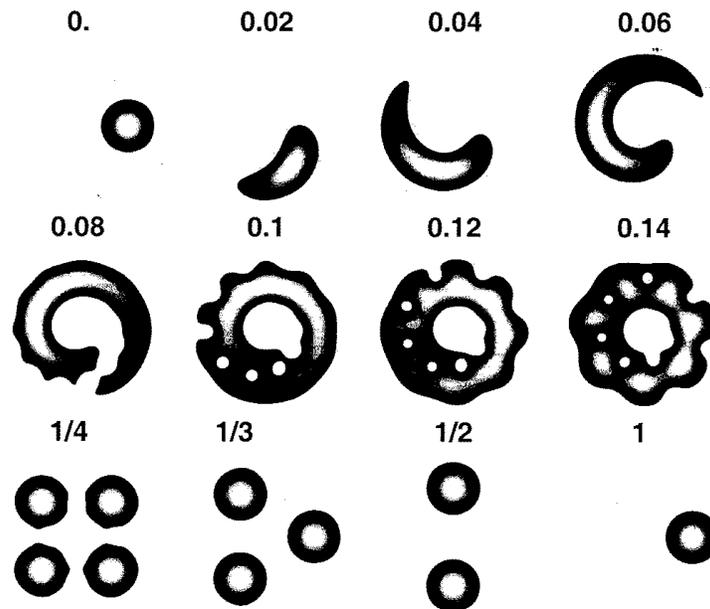

Figure 1. Contour plot of the Q function $|\langle\beta|\alpha(t)\rangle|^2/\pi$ of an initially coherent state $|\alpha\rangle$ propagating through a Kerr medium. The horizontal and vertical axes represent respectively the real and imaginary parts of β. The plots are labeled by their time values (in units of the revival time).

which allows us to write

$$|\alpha(t)\rangle = \int \frac{\mathrm{d}^2\beta}{\pi}|\beta\rangle\langle\beta|\alpha(t)\rangle. \tag{12}$$

Thus the probability of $|\alpha(t)\rangle$ being in a coherent state $|\beta\rangle$ is given by $|\langle\beta|\alpha(t)\rangle|^2/\pi$ which is the Q function. In figure 1, we plot the time evolution of the Q function as a function of the real and imaginary parts of β. Note that at $t = 0$, the Q function is a Gaussian, $Q(0) = \exp(-|\alpha - \beta|^2)/\pi$, peaked at $\beta = \alpha$. For $t \ll$ the revival time $T = \pi/\chi$, the Q function spreads along the perimeter of a circle of radius $|\alpha|$ until the head meets the tail. Thereafter it begins to break up into bits and at fractions of the revival time, it produces replicas of the initial Q function. Can we observe these things? There is good news and bad news. The good news is that the Q functions can be measured by eight-port homodyne detectors [16]. The bad news is that in the present example, χ is a very small quantity which makes the revival time $T = \pi/\chi$ (and hence the revival length) too large for the experiment to be feasible.

3. Generalisations

The above example was somewhat special in that the initial state was a coherent state which was expanded in terms of number states that were eigenfunctions of the Hamiltonian H. The energy eigenvalues $E_n = \chi(n^2 - n)$ were quadratic in n. We have seen that it is the quadratic term in E_n that was responsible for cat formation. How can we generalise this result?

Let us consider a more complicated Hamiltonian $H = f(a^\dagger a) = \sum_k \beta_k (a^\dagger a)^k$ and let the initial state be given by $|\Psi(0)\rangle = \sum_n \phi_n|n\rangle$. Then the state at time t has the form

$$|\Psi(t)\rangle = \sum_n \phi_n \exp[-itf(n)]|p\rangle. \tag{13}$$

If the amplitude ϕ_n is sufficiently peaked about $n = n_0$, *then* one can expand the energy eigenvalue $f(n)$ in a Taylor series about $n = n_0$ and drop the higher order terms:

$$f(n) = f_0 + (n - n_0)f_0' + \frac{(n - n_0)^2}{2}f_0'' + \cdots. \tag{14}$$

In this way, one can recover a quadratic energy eigenvalue even for a more general Hamiltonian. Thus, both the non-linearity of H and the peaked nature of the initial wave packet are needed for the formation of Schrödinger cats.

Of course, the basis functions need not be number states. A classic example is the case of Rydberg atoms. Here, the basis functions are the negative energy solutions of the Schrödinger equation for the Coulomb potential. The energy eigenvalues E_n have the highly nonlinear n^{-2} dependence. But for Rydberg wave packets, the energy levels are close enough so that the spread $\Delta n = |n - n_0|$ is much less than n_0, the mean value about which the levels are chosen. This makes it possible to expand E_n about $n = n_0$ in a Taylor series and approximate it as a quadratic polynomial in n. No wonder, then, that the Rydberg wave packets have proved to be fertile ground for the study of fractional revivals in quantum systems [2].

There are two other ways we can extend our previous result: (a) we can consider two-mode systems for which the Hamiltonian has the form $H = f(a^\dagger a, b^\dagger b)$; (b) we can also consider, as our initial state, coherent states of other symmetry groups such as SU(1,1) and SU(2).

4. Two-mode systems and their evolution

The Q function for two-mode cases will be four-dimensional and difficult to visualize. So, we will look at the evolution of quadrature distributions instead. The quadrature distribution for a state vector $|\psi(t)\rangle$ is defined as $|\psi(x, y, t)|^2 = |\langle x, y|\psi(t)\rangle|^2$, where $|x, y\rangle$ is the eigenvector of $(a + a^\dagger)/\sqrt{2}$ and $(b + b^\dagger)/\sqrt{2}$ with eigenvalues x and y respectively. Quadrature distributions can be measured by homodyne method [16]. We have studied the wave packet dynamics of two-mode coherent states under the action of a generic, phase insensitive Hamiltonian (we use $\hbar = 1$):

$$H = c_1 \left[(a^\dagger a)^2 + (b^\dagger b)^2 \right] - c_2 a^\dagger a b^\dagger b. \tag{15}$$

Setting $T_\pm = \pi/(2c_1 \pm c_2)$, the Hamiltonian can be readily diagonalised:

$$H = \frac{\pi}{4} \left[(a^\dagger a + b^\dagger b)^2/T_- + (a^\dagger a - b^\dagger b)^2/T_+ \right]. \tag{16}$$

4.1 *HO coherent states*

Two-mode HO coherent states can be written in terms of two-mode number states in the following way:

$$|\alpha, \beta\rangle = \sum_{m,n} C_{mn}|m, n\rangle \quad m, n = 1, 2, 3, \ldots \infty. \tag{17}$$

We construct the even (+) and odd (−) states

$$|\alpha, \beta\rangle_\pm = |\alpha, \beta\rangle \pm |-\alpha, -\beta\rangle) \tag{18}$$

which have number state expansions in the form

$$|\alpha, \beta\rangle_+ = \sum_{p,q} C_{pq}^{(+)}|2p, 2q\rangle + D_{pq}^{(+)}|2p + 1, 2q + 1\rangle \tag{19}$$

$$|\alpha, \beta\rangle_- = \sum_{p,q} C_{pq}^{(-)}|2p, 2q + 1\rangle + D_{pq}^{(-)}|2p + 1, 2q\rangle. \tag{20}$$

Our major findings [17] on the evolution of their quadrature distribution are as follows: (a) In the short-term, the nonlinearity of the Hamiltonian destroys the initial coherence, and the patterns are similar for both even and odd states (see figure 2); whereas (b) the long-term evolution guarantees revival and fractional revival of the initial state but depends crucially on the ratio T_+/T_- and on the symmetry of the initial state. The even and odd states evolve quite differently in the long term and *the even state takes twice as long to revive as the odd state* (see figure 3).
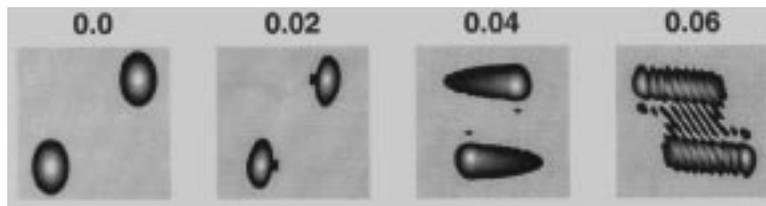
Figure 2. Contour plots of the quadrature distributions for $|\alpha, \beta\rangle_-$ at different times for $\alpha = 2$, $\beta = 3$ and $T_+/T_- = 2/3$. The plots are labeled by their time values (in units of T_-). Notice how the initial coherent structure is quickly eroded. Furthermore, the corresponding plots for $|\alpha, \beta\rangle_+$ are the same (in the scale of the plots).
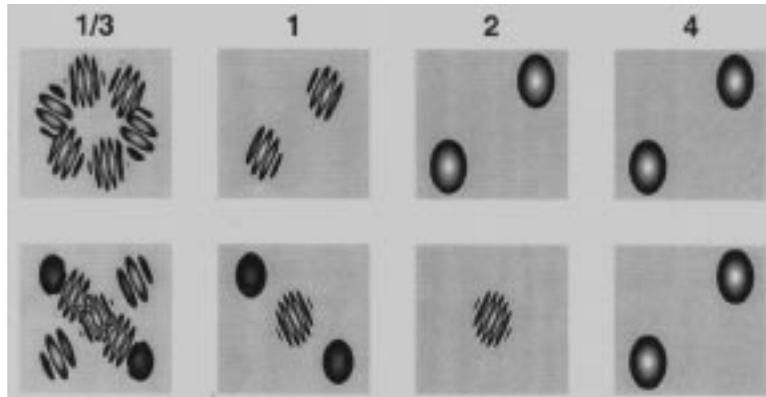

Figure 3. Contour plots of the quadrature distributions for $|\alpha, \beta\rangle_-$ (top row) and $|\alpha, \beta\rangle_+$ (bottom row) at later times. All other parameters are as in figure 2.

4.2 *SU(1,1) coherent states*

SU(1,1) states arise in nonlinear parametric processes where photons are either created or destroyed in pairs so that in a two-mode (a, b) system, the photon number difference $q = a^\dagger a - b^\dagger b$ is an integer constant.

How do we define SU(1,1) *coherent* states? It is possible to suitably generalise any of the three defining properties of a HO coherent state to realize coherent states of the SU(1,1) group. But the outcomes are not equivalent to one another. Thus, the action of the SU(1,1) squeeze operator on the vacuum state produces the so-called Perelomov [11] coherent states, the eigenstates of the lowering operator element of the SU(1,1) algebra are the Barut–Giradello [18] or pair coherent states [10], and equalized (rather than minimum) uncertainty states are called 'intelligent' SU(1,1) states [19]. Here, we adopt a unifying approach [12,13] which unites all these three definitions by defining the SU(1,1) coherent states to be the minimum uncertainty states with equal variance in two orthogonal variables. These are superpositions of number states of the form $|n + q, n\rangle$ where $n = 0, 1, 2, \ldots, \infty$:
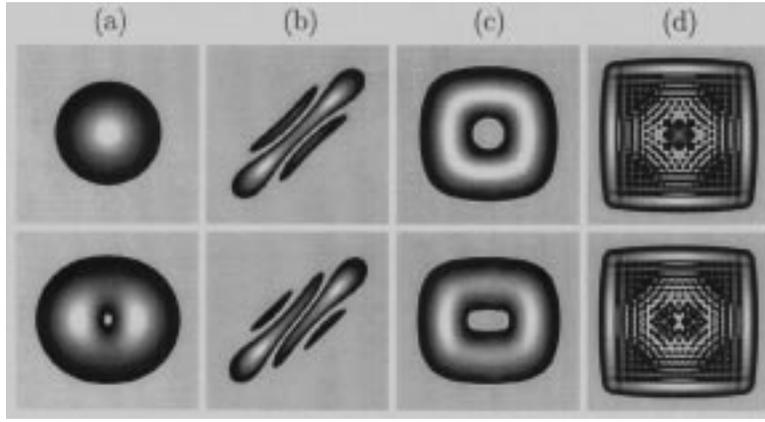
Figure 4. Contour plots of the quadrature distribution at $t = 0$ for the SU(1,1) coherent state $|\psi(\eta, \xi, 0)\rangle$ (top row) and $|\psi(\eta, \xi, 1)\rangle$ (bottom row) when (**a**) $\eta = -i \tanh \pi/4$, $\xi = 0$; (**b**) $\eta = 0$, $\xi = 3$; (**c**) $\eta = 0$, $\xi = -3i$; (**d**) $\eta = -i \tanh 2\pi/5$, $\xi = 3i$. Note that case (a) is a Perelomov coherent state, cases (b) and (c) represent pair coherent states whereas case (d) is more general.

$$|\eta, \xi, q\rangle = N(\xi, q) \exp(-\xi \eta^*)$$
$$\times \sum_{n=0}^{\infty} \frac{\xi^n (1 - |\eta|^2)^{n + \frac{q+1}{2}} \sqrt{(n+n')!(n+n'+q)!}}{n!(n+q)!} |n + n' + q, n + n'\rangle, \quad (21)$$

where

$$N(\xi, q) = \left[\sum_{n=0}^{\infty} \frac{|\xi|^{2n}}{n!(n+q)!} \right]^{-1/2}. \quad (22)$$

For pair coherent states $\eta \to 0$ whereas for Perelomov coherent states $\xi \to 0$. Since η and ξ are continuous and (in general) complex parameters, infinitely many other cases of $|\eta, \xi, q\rangle$ exist even for the same value of q. Some illustrative examples are shown in figure 4. For SU(1,1) coherent states, $q = a^\dagger a - b^\dagger b$ being constant, it is clear from eq. (16) that T_+ and hence the ratio T_-/T_+ does not play an active role in the evolution of these states. However, the parity of q was found to be crucial in determining the revival features of SU(1,1) coherent states. Thus for odd values of q, the quadrature distribution is revived at all integer values of T_-. This is so for even values of q as well only when ξ and η are pure imaginary. In general, however, the quadrature distribution for even values of q is revived at *even* multiples of T_-. In figure 5, we show how the quadrature distribution of a pair coherent state (with $\xi = 3$ and $q = 0$) evolves in time.

4.3 *SU(2) coherent states*

SU(2) states can be produced in parametric processes in which a 'photon' in mode a is created at the expense of a 'photon' in mode b, and vice-versa keeping the total number of
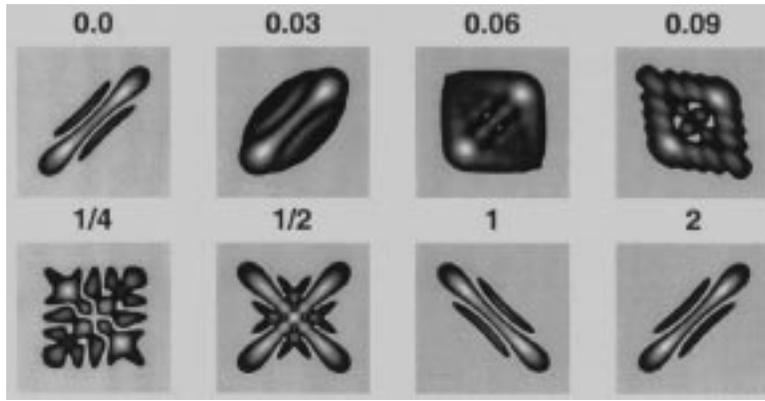
Figure 5. Contour plots of the quadrature distributions for a pair coherent state ($\xi = 3$, $q = 0$, $\eta = 0$) at different times. The plots are labeled by their time values t (in units of T_-). Note how the initial coherent structure is lost quickly, but is regained later on to form a Schrödinger cat at $t = 1/2$ and eventually to experience full revival at $t = 2$.

photons $N = a^\dagger a + b^\dagger b$ constant. The word 'photon' is placed under quotes to mean that one of the modes can, in fact, represent something other than a light field. A celebrated example is the interaction of a system of N two-level atoms with a single-mode (represented by its annihilation operator a) near-resonant radiation field. The field will induce transitions between the two levels. Let b and c be the annihilation operators of the atom in the excited and ground states respectively. Then an interaction term of the form $ab^\dagger c$ will excite a single atom to the upper level thus depleting both the ground state population and the available number of photons by unity. In parametric approximation, the ground state population is sufficiently large so that its depletion is ignored (i.e., c is treated as a c-number). Let us now assume that all the atoms are initially in the ground state. Let the atomic system interact with the radiation field up to a time t_1 and then evolve freely up to the time t_2. The final state will be an SU(2) coherent state.

The SU(2) coherent state can be constructed (defined) in ways similar to the SU(1,1) coherent state. One can also form a generalized SU(2) coherent state. Here however, we have chosen to define the SU(2) coherent state in the Perelomov sense, that is, by shifting the vacuum state with a unitary operator. In the Schwinger representation of the SU(2) algebra [14], SU(2) coherent states $|\tau, N\rangle$ are formed by the superposition of number states of the form $|K, N - K\rangle$ where $N = a^\dagger a + b^\dagger b$ is an integer constant and $K = 0, 1, 2, \ldots,$ N:

$$|\tau, N\rangle = \left(1 + |\tau|^2\right)^{-N/2} \sum_{K=0}^{N} \left(\begin{array}{c} N \\ K \end{array} \right)^{1/2} \tau^K |K, N - K\rangle. \tag{23}$$

The parameter τ is, in general, complex and has a physical meaning in that $|\tau|^2$ is the ratio of the mean number of photons in the two modes.

Although the probability of finding K bosons in one mode is clearly seen to be binomial, it should be noted that the photon distribution in each mode has sub-Poissonian statistics. To see this, we evaluate Mandel's Q parameter Q_1 (for the first mode) and Q_2 (for the second mode) and find
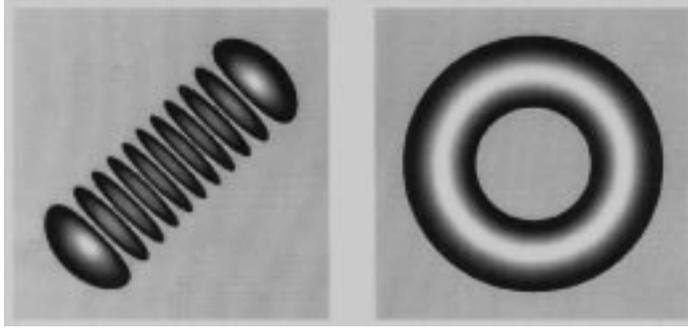
Figure 6. Contour plots of the quadrature distributions for the SU(2) coherent state $|\tau, 10\rangle$ for $\tau = 1$ (left picture) and $\tau = i$ (right picture).
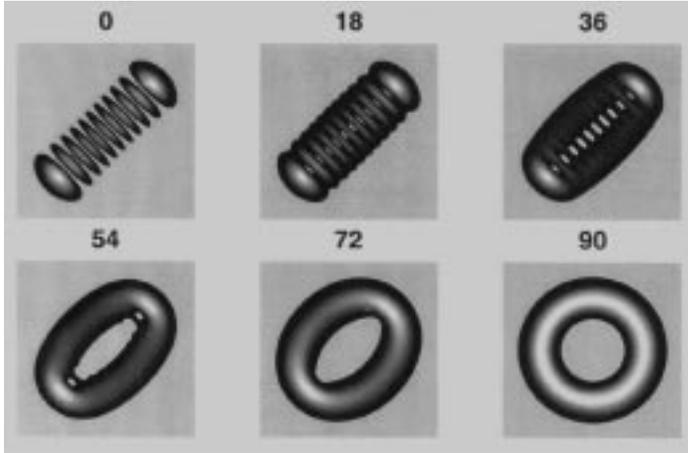

Figure 7. Contour plots of the quadrature distributions for the SU(2) coherent state $|e^{i\chi}, 11\rangle$ for different values of the phase χ. The plots are labeled by their phase values (in degrees).

$$Q_1 = -\frac{|\tau|^2}{1 + |\tau|^2}, \quad Q_2 = -\frac{1}{1 + |\tau|^2}. \tag{24}$$

The SU(2) coherent states given by eq. (23) are represented by the wave function

$$\psi(x, y, 0) = \frac{1}{\sqrt{\pi 2^N N!}} \left[\frac{1 + \tau^2}{1 + |\tau|^2}\right]^{N/2} e^{-(x^2 + y^2)/2} H_N\left(\frac{\tau x + y}{\sqrt{1 + \tau^2}}\right). \tag{25}$$

Clearly the corresponding quadrature distribution will depend not only on N but also on the amplitude and phase of the parameter τ. The distribution, which is a Gaussian modulated by the square of a Hermite polynomial, will have dark fringes at the nodes of the latter and will be lined up at an angle $\tan^{-1}(1/\tau)$ with respect to the positive x-axis. For $\tau = \pm 1$, the distribution is along the diagonals $x = \mp y$. An altogether different pattern arises in the limiting case $\tau \to \pm i$. One obtains a wave function with vortex structure:
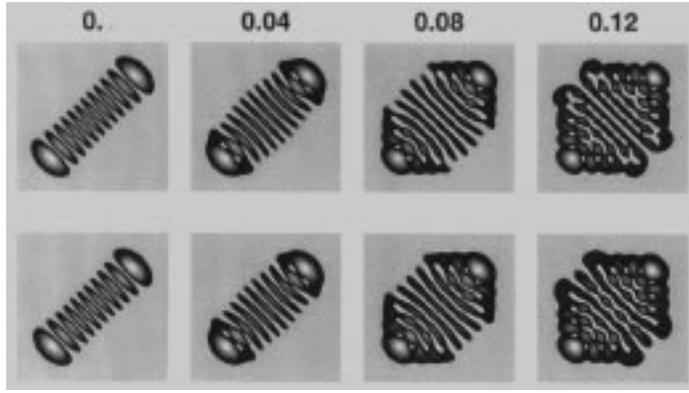
Figure 8. Contour plots of the quadrature distributions for the SU(2) coherent state $|1, N\rangle$ as a function of time for $N = 11$ (top row) and $N = 10$ (bottom row). The plots are labeled by their time values (in units of T_+).
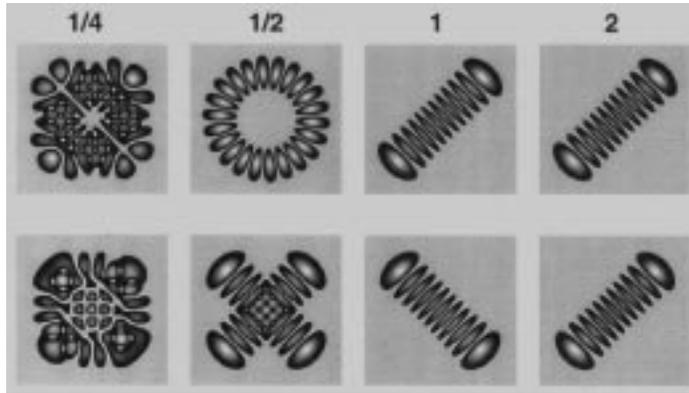

Figure 9. As in figure 8, but at later times.

$$\psi(x, y, 0)|_{\tau=\pm i} = \frac{(x^2 + y^2)^{N/2}}{\sqrt{\pi N!}} e^{-\frac{x^2+y^2}{2} \pm iN\eta}, \quad \eta = \tan^{-1}\left(\frac{x}{y}\right). \qquad (26)$$

The quadrature distributions corresponding to $\tau = 1$ and $\tau = i$ are shown in figure 6. The remarkable transition from one pattern to another can be realized by setting $\tau = e^{i\chi}$ and changing the phase χ from zero to 90 degrees. This is shown in figure 7 for $N = 10$. For $N \gg 1$, the quadrature distributions of $|\tau, N\rangle$ and $|\tau, N+1\rangle$ will have similar initial patterns and short-time evolutions (see figure 8). But their long-time evolutions and revival features (see figure 9) will depend critically on the parity of N. In fact, one can show that under the action of the Hamiltonian H given by eq. (16), $|\tau, N\rangle$ revives (but for an over-all phase factor) at *all* integer multiples of T_+ if N is odd, and at *even* multiples of T_+ if N is even. If τ is pure imaginary, then the revival time is the same for *all* values of N. Fractional revivals (if any) will occur at times $t = (r/s)T_+$, where r and s are mutually prime with $r < s$.

As an illustration of fractional revival and cat formation, we explain the patterns obtained at $t = T_+/2$ (see figure 9). If $\mathcal{U}(t) = \exp(-iHt)$ is the time evolution operator, then one can show that

$$\mathcal{U}(T_+/2)|1, 10\rangle \rightarrow |-1, 10\rangle + i|1, 10\rangle, \tag{27}$$

$$\mathcal{U}(T_+/2)|1, 11\rangle \rightarrow |-i, 11\rangle + i|i, 11\rangle. \tag{28}$$

The wave functions corresponding to $|\pm 1, N\rangle$ are real (see eq. (25)). In eq. (27), these state vectors are added with a $\pi/2$ phase difference yielding a cat state whose quadrature distribution is an incoherent sum of the distributions for $|1, 10\rangle$ and $|-1, 10\rangle$. In eq. (28), on the other hand, the state vectors $|\pm i, N\rangle$ are added with a $\pi/2$ phase difference. But the wave functions for $|\pm i, N\rangle$ are complex (see eq. (26)) giving rise to strong interference. The quadrature distribution for $\mathcal{U}(T_+/2)|1, 11\rangle$ is found to be

$$(1 - \sin 2\eta N) \times \text{the quadrature distribution for } |\pm i, N\rangle,$$

where $N = 11$ and $\eta = \tan^{-1}(x/y)$. Dark fringes will appear whenever $\sin 2\eta N = 1$, i.e. $\eta = (m + 1/4)\pi/N$ where m is an integer. Since $0 \leq \eta \leq 2\pi$, the total number of such fringes will be $2N$. Although there will also be $2N$ bright patches, the phenomenon is *not* a $2N$-way fractional revival. Rather, it is more like *'slicing a doughnut'* radially in $2N$ equal parts.

5. The odd-even paradox – a simple explanation

There is no problem, no matter how complicated, which, when viewed in the correct light, does not appear more complicated – Piers Anthony

An interesting and recurring aspect of this work is the observation that the revival time for 'even' states is, in general, twice as long as for 'odd' states. In the following we give a simple explanation as to why this is so.

Recall that the two-mode HO coherent states were described as even (odd) if they were composed of Fock states $|m, n\rangle$ where m and n have (same) different parity (see eqs (19) and (20)). For SU(1,1) coherent states, the parity of the photon number difference $q = a^\dagger a - b^\dagger b$ determines whether the state in question is even or odd. Finally, SU(2) coherent states are described as even or odd depending on whether the total number of photons $N = a^\dagger a + b^\dagger b$ is even or odd respectively.

In each case, the time evolution of the quadrature distribution involves sums of the form

$$f(t) = \sum_p c_p \exp\{-2\pi i p^2 (t/T)\}. \tag{29}$$

The summation index p runs through even (odd) integer values for even (odd) states. One can now easily show that for odd states $f(T/8) = f(0)$ (but for an over-all phase factor) whereas for even states $f(T/4) = f(0)$. Thus the revival time for even states is twice that of odd states.

6. Conclusion

In conclusion, we have given a brief introduction to coherent states of various symmetry groups and compared the non-linear wave packet dynamics of their two-mode realizations. In each case, the initial coherent structure is lost quickly but is regained later on to experience the quantum phenomenon of revival and the formation of Schrödinger cats. We have also shown that the parity of the initial state determines the long-time dynamics.

References

[*] For a set of movies on this topic, see J Banerji and G S Agarwal, *Opt. Express* **5**, 220 (1999)

[1] Such revivals have been studied extensively in Rydberg atoms (see ref. [2]), in optical parametric oscillators (see ref. [3]), in the Jaynes–Cummings model (see ref. [4]) and also, in a general way, in the temporal behavior of generic transient signals originating from multilevel quantum systems (see ref. [5]). See also the recent papers on square well potentials
D L Aronstein and C Stroud, *Phys. Rev.* **A55**, 4526 (1997)
F Grobmann, J M Rost and W P Schleich, *J. Phys.* **A30**, L277 (1997)

[2] I Sh. Averbukh and N F Perelman, *Phys. Lett.* **A139**, 449 (1989)
M Nauenberg, *J. Phys.* **B23**, L385 (1990)
G Alber, H Ritsch and P Zoller, *Phys. Rev.* **A34**, 1058 (1986)
Z D Gaeta and C R Stroud Jr., *Phys. Rev.* **42**, 6308 (1990)
R Bluhm, V Alan Kostelecky and B Tudose, *Phys. Rev.* **52**, 2234 (1995); **53**, 937 (1996)

[3] I V Jyotsna and G S Agarwal, *J. Mod. Opt.* **44**, 305 (1997)
G S Agarwal and J Banerji, *Phys. Rev.* **A55**, R4007 (1997)
G Drobny and I Jex, *Phys. Rev.* **45**, 1816 (1992)

[4] J H Eberly, N B Narozhny and J J Sanchez-Mondragon. *Phys. Rev. Lett.* **44**, 1323 (1980)
P L Knight and B W Shore, *Phys. Rev.* **A48**, 642 (1993)
G Rempe, H Walther and N Klein, *Phys. Rev. Lett.* **58**, 353 (1987)

[5] C Leichtle, I Sh Averbukh and W P Schleich, *Phys. Rev.* **A54**, 5299 (1996)

[6] Fractional revivals have been observed experimentally in the motion of atomic Rydberg wave packets
J A Yeazell and C R Stroud, *Phys. Rev.* **A43**, 5153 (1991)
D R Meacher, P E Meyler, I G Hughes and P Ewart, *J. Phys.* **B24**, L63 (1991)
J Wals, H H Fielding, J F Christian, L C Snoek, W J van der Zande and H B van Linden van den Heuvell, *Phys. Rev. Lett.* **72**, 3783 (1994) and in molecular vibrational wave packets
M J J Vrakking, D M Villeneuve and A Stolow, *Phys. Rev.* **A54**, R37 (1996)

[7] B Yurke and D Stoler, *Phys. Rev. Lett.* **57**, 13 (1986)
G J Milburn and C A Holmes, *Phys. Rev. Lett.* **56**, 2237 (1986)
W Schleich, M Pernigo and Fam Le Kien, *Phys. Rev.* **A44**, 2172 (1991)
K Tara, G S Agarwal and S Chaturvedi, *Phys. Rev.* **47**, 5024 (1993)
V Bužek, H Moya-Cessa and P L Knight, *Phys. Rev.* **45**, 8190 (1992)
R Tanaś, Ts Gantsog, A Miranowicz and S Kielich, *J. Opt. Soc. Am.* **B8**, 1576 (1991)
G C Gerry, *Opt. Commun.* **63**, 278 (1987)

[8] D L Aronstein and C Stroud, *Phys. Rev.* **A55**, 4526 (1997)
F Grobmann, J M Rost and W P Schleich, *J. Phys.* **A30**, L277 (1997)

[9] M J J Vrakking, D M Villeneuve and A Stolow, *Phys. Rev.* **A54**, R37 (1996)

[10] G S Agarwal, *J. Opt. Soc. Am.* **B5**, 1940 (1988)

[11] A M Perelomov, *Generalized coherent states and their applications* (Springer, Berlin 1986);
Coherent states edited by J R Klauder and B S Skagerstam (World Scientific, Singapore, 1985)
C M Caves and B L Shumaker, *Phys. Rev.* **A31**, 3068, 3093 (1985)

[12] J Banerji and G S Agarwal, *Phys. Rev.* **A59**, 4777 (1999)

[13] R R Puri and G S Agarwal, *Int. J. Mod. Phys.* **B10**, 1563 (1996); *Phys. Rev.* **A53**, 1786 (1996)
For earlier work on SU(1,1) coherent and squeezed states, see Satya Prakash and G S Agarwal,
Phys. Rev. **A50**, 4258 (1994); **52** (1995)
C C Gerry and R Grobe, *Phys. Rev.* **A51**, 4123 (1995)

[14] K Wódkiewicz and J H Eberly, *J. Opt. Soc. Am.* **B2**, 458 (1985)
V Bužek and T Quang, *J. Opt. Soc. Am.* **B6**, 2447 (1989)
A Luis and J Peřina, *Phys. Rev.* **A53**, 1886 (1996)
G S Agarwal, R R Puri and R P Singh, *Phys. Rev.* **A56**, 2249 (1997)

[15] J H Hannay and M V Berry, *Physica* **D1**, 267 (1980)

[16] U Leonhardt, *Measuring the quantum state of light* (Cambridge Univ. Press, Cambridge, 1997)

[17] Details are to be found in G S Agarwal and J Banerji, *Phys. Rev.* **A57**, 3880 (1998)

[18] A O Barut and L Girardello, *Commun. Math. Phys.* **21**, 41 (1971)

[19] C C Gerry and R Grobe, *Phys. Rev.* **A51**, 4123 (1995)